

# Coherent $c$ -axis transport in the underdoped cuprate superconductor $\text{YBa}_2\text{Cu}_3\text{O}_y$

B. Vignolle,<sup>1</sup> B. J. Ramshaw,<sup>2</sup> James Day,<sup>2</sup> David LeBoeuf,<sup>1</sup> Stéphane Lepault,<sup>1</sup>  
Ruixing Liang,<sup>2,3</sup> W.N. Hardy,<sup>2,3</sup> D.A. Bonn,<sup>2,3</sup> Louis Taillefer,<sup>3,4</sup> and Cyril Proust<sup>1,3,\*</sup>

<sup>1</sup>*Laboratoire National des Champs Magnétiques Intenses,  
UPR 3228, (CNRS-INSU-UMR-UPS), Toulouse 31400, France*

<sup>2</sup>*Department of Physics and Astronomy, University of British Columbia, Vancouver V6T 1Z4, Canada*

<sup>3</sup>*Canadian Institute for Advanced Research, Toronto M5G 1Z8, Canada*

<sup>4</sup>*Département de physique & RQMP, Université de Sherbrooke, Sherbrooke, Québec J1K 2R1, Canada*  
(Dated: July 28, 2011)

The electrical resistivity  $\rho_c$  of the underdoped cuprate superconductor  $\text{YBa}_2\text{Cu}_3\text{O}_y$  was measured perpendicular to the  $\text{CuO}_2$  planes on ultra-high quality single crystals in magnetic fields large enough to suppress superconductivity. The incoherent insulating-like behavior of  $\rho_c$  at high temperature, characteristic of all underdoped cuprates, is found to cross over to a coherent regime of metallic behavior at low temperature. This crossover coincides with the emergence of the small electron pocket detected in the Fermi surface of  $\text{YBa}_2\text{Cu}_3\text{O}_y$  via quantum oscillations, the Hall and Seebeck coefficients and with the detection of a unidirectional modulation of the charge density as seen by high-field NMR measurements. The low coherence temperature is quantitatively consistent with the small hopping integral  $t_\perp$  inferred from the splitting of the quantum oscillation frequencies. We conclude that the Fermi-surface reconstruction in  $\text{YBa}_2\text{Cu}_3\text{O}_y$  at dopings from  $p = 0.08$  to at least  $p = 0.15$ , attributed to stripe order, produces a metallic state with 3D coherence deep in the underdoped regime.

PACS numbers: 74.25.Bt, 74.25.Ha, 74.72.Bk

Understanding the behavior of the interplane  $c$ -axis transport in the underdoped, high-transition-temperature (high- $T_c$ ), cuprate superconductors is of crucial importance to elucidate the normal state properties of these materials [1, 2]. While the in-plane resistivity is metallic down to  $T_c$  in many underdoped cuprates, the inter-plane resistivity along the  $c$ -axis is insulating-like [3]. The peculiar properties of  $c$ -axis charge transport are demonstrated by  $c$ -axis optical conductivity measurements by the absence of a Drude peak at low frequencies in the underdoped normal state above  $T_c$  [4]. This behavior of the  $c$ -axis charge transport has been ascribed to the opening of the pseudogap and the lack of a well-defined quasiparticle peak in those regions of momentum space that control inter-plane transport [5], but theoretical models differ as to whether the ground state is insulating [6] or metallic (see ref 7 and ref. therein). In order to understand  $c$ -axis transport in cuprates, an important new experimental fact must be taken into account: the Fermi surface (FS) of underdoped cuprates undergoes a profound transformation at low temperature, as revealed by the observation of quantum oscillations [8]. Combined with the negative Hall [9] and Seebeck coefficients [10] at low temperature, these measurements demonstrate that the FS of underdoped  $\text{YBa}_2\text{Cu}_3\text{O}_y$  is made of small electron pockets in contrast to the large, hole-like FS of the overdoped cuprates [11]. de Haas-van Alphen [12] and tunnel diode oscillation [13] (TDO) measurements in underdoped  $\text{YBa}_2\text{Cu}_3\text{O}_y$  revealed the presence of multiple frequencies, which have been interpreted as bi-layer splitting and warping of the FS effect in one case [12, 14][38] and as compensated electron and hole pockets in another

[13]. Quantum oscillations cannot give direct information on the sign and the location of the FS but interpreting the splitting of the frequency as warping of the FS leads to a hopping integral,  $t_\perp$ , of order of 15 K [12] (1.3 meV). This value is one order of magnitude smaller than the value of the inter-bi-layer hopping predicted by band structure calculations [15], which overestimates the transfer integral between layers ( $t_\perp \approx 30$  meV) and therefore predict a metallic-like  $c$ -axis resistivity, even at high temperature. The small  $t_\perp$  deduced from quantum oscillations implies that quasiparticle motion in the inter-plane direction should be coherent at temperatures lower than  $t_\perp/k_B$ , contrary to the current belief. Here we directly address the possibility of coherent motion between  $\text{CuO}_2$  planes by measuring the  $c$ -axis resistivity at low temperature in magnetic fields large enough to suppress superconductivity.

We found that the  $c$ -axis resistivity becomes metallic-like at low temperature, and interpret this as a consequence of  $c$ -axis coherence. The low coherence temperature implies a small  $c$ -axis dispersion and therefore a small  $t_\perp$ , in quantitative agreement with the splitting of the multiple quantum oscillation frequencies [12, 14]. The onset of this crossover coincides with the emergence of an electron pocket, as inferred from the change of sign of the Hall [9, 16] and Seebeck [10, 17] coefficients at low temperature, and concomitant with the onset of a unidirectional modulation of the charge density observed in recent NMR measurements [18]. This high mobility pocket produces metallic-like transport both in the plane [16] and along the  $c$ -axis. Since  $c$ -axis transport is mostly dominated by the anti-nodal states [19], the coherent be-

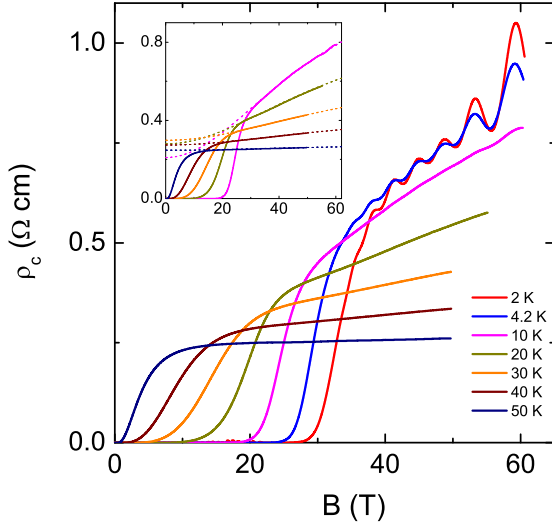


FIG. 1: (color on line) Electrical resistivity  $\rho_c$  of  $\text{YBa}_2\text{Cu}_3\text{O}_y$  ( $p=0.109$ ) for a current  $I$  and a magnetic field  $B$  along the  $c$  axis ( $I \parallel B \parallel c$ ) at different temperatures below  $T_c$ . Inset: Same data between 10 K and 50 K with a fit of each isotherm (dashed lines) using a two-band model above the superconducting transition.

haviour and the large amplitude of the quantum oscillations in the  $c$ -axis resistivity suggest that they arise from anti-nodal states. The coherence temperature decreases as the doping level decreases and vanishes at a hole doping  $p \approx 0.08$ , corresponding to the doping level where the electron pocket disappears [16]. In the absence of the electron pocket, transport along  $c$ -axis remains incoherent.

Fig. 1 presents the longitudinal  $c$ -axis resistivity up to 60 T for an underdoped sample of  $\text{YBa}_2\text{Cu}_3\text{O}_y$  ( $T_c=61.3$  K,  $p=0.109$ ). Data for two other compositions ( $p=0.097$  and  $0.12$ ) are shown in the supplementary material [20]. Below 60 K, a strong positive magnetoresistance (MR) grows with decreasing temperature, in good agreement with earlier high-field measurements [21] of  $\rho_c$  on  $\text{YBa}_2\text{Cu}_3\text{O}_y$  crystals with  $T_c = 60$  K. At very low temperature, strong quantum oscillations can clearly be seen, arising from the quantization of cyclotron orbits perpendicular to the magnetic field. The frequencies and temperature dependence of these oscillations are consistent with previous reports [8, 12–14]. Two features common to all three samples are the rise of the in-field  $c$ -axis resistivity down to about 4 K, and the clear saturation at lower temperature. This behavior is best captured in Fig. 2 where the resistivities measured at zero field (solid line) and at  $B = 50$  T (green open squares) are compared with the insulating-like high temperature behavior, where the  $c$ -axis resistivity follows a  $1/T$  dependence (dashed line in Fig. 2). The inset of Fig. 2 makes it evident that the saturation of  $\rho_c(T)$ , at low temperature and for a given field above 50 T, is

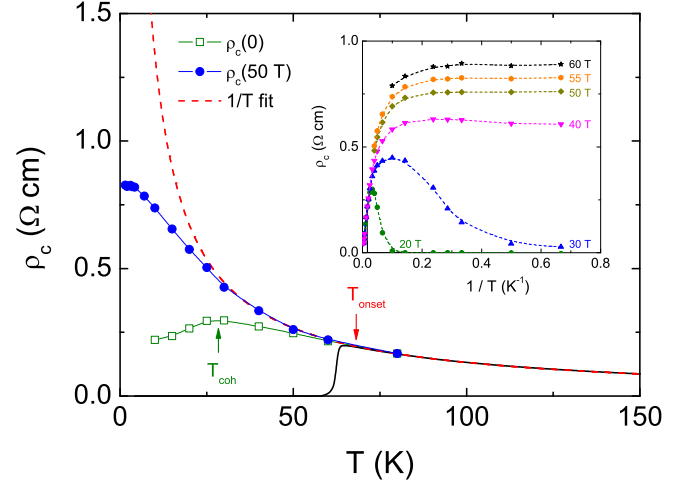


FIG. 2: (color on line) Temperature dependence of the  $c$ -axis resistivity of  $\text{YBa}_2\text{Cu}_3\text{O}_y$  ( $p=0.109$ ) measured at zero magnetic field (black solid line) and at  $B = 50$  T (blue circles). Dashed line is a  $1/T$  fit to the high temperature data up to 300 K. The saturation of the in-field resistivity at low temperature contrasts with the insulating-like behavior seen at high temperature. The green open squares correspond to the resistivity from which the magnetoresistance has been subtracted using a two-band model to extrapolate the normal-state data of Fig. 1 to  $B = 0$  (see [20]). The inset shows data of Fig. 1 plotted as a function of  $1/T$  for different values of the magnetic field. Dashed lines are a guide to the eye.

not due to some compensation between superconducting drop (as seen for the data below 40 T) and insulating-like normal-state resistivity since the saturation persists at fields higher than 50 T. From Nernst, in-plane and out-of-plane transport measurements [20], the threshold field above which there is negligible flux-flow contribution to the resistivity was identified; at all three dopings, 50 T is above this threshold field down to the lowest temperatures. The magnetoresistance measured at 50 T is purely a normal-state property at all three dopings. Consequently, in fields of 50 T and above, where the  $c$ -axis resistivity saturates as  $T \rightarrow 0$ , the non-superconducting ground state of  $\text{YBa}_2\text{Cu}_3\text{O}_y$  is coherent in all three directions at  $p = 0.10 - 0.12$ .

The observation of  $c$ -axis coherent transport implies that charge carriers are not confined to the  $\text{CuO}_2$  planes [2] and that coherent Bloch bands along the  $c$ -axis form at low temperature. While there is no doubt about the existence of a three-dimensional Fermi surface in overdoped cuprate superconductors [22], our findings suggest that inter-plane transport in underdoped  $\text{YBa}_2\text{Cu}_3\text{O}_y$  can also, in principle, be described at low temperature within the same conventional theory of metals. In this case, the  $c$ -axis conductivity is given by  $\sigma_c = \frac{4e^2 c t_\perp^2 m^* \tau_c}{\pi \hbar^4}$  where  $c$  is the  $c$ -axis lattice parameter,  $\tau_c$  is the relaxation time, and  $m^*$  is the effective mass. For a tetragonal cuprate material, the interlayer hopping inte-

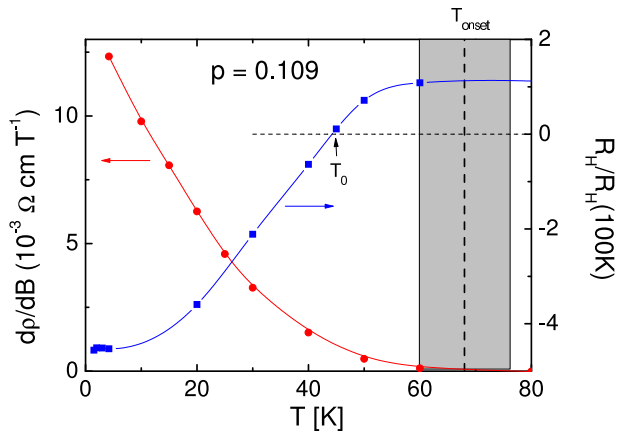


FIG. 3: (color on line) The slope of the  $c$ -axis magnetoresistance evaluated at  $B = 50$  T (red circles; left axis) and in-plane Hall coefficient  $R_H$  (blue squares; right axis) of  $\text{YBa}_2\text{Cu}_3\text{O}_y$  ( $p=0.108$ ) as a function of temperature.  $R_H$  data measured at  $B = 54$  T is taken from ref. 16 and normalized by its value at  $T = 100$  K.  $T_0$  is the temperature at which  $R_H(T)$  changes sign from positive at high temperature to negative at low temperature [9, 16].  $T_{\text{onset}}$  is the temperature below which  $\rho_c(T)$  deviates downward from its  $1/T$  dependence at high temperature (vertical dashed line).

gral  $t_\perp$  depends strongly on the in-plane momentum  $\mathbf{k}$  of carriers, namely [23] :  $t_\perp(\mathbf{k}) = \frac{t_\perp^0}{4}[\cos(k_x a) - \cos(k_y b)]^2$ . It is maximum at the anti-node i.e. at the  $(\pi, 0)$  (and equivalent) points in the Brillouin zone. The coherent  $c$ -axis transport we observe at low temperature can be interpreted in two different ways. Assuming that electronic states exist only at the node and considering the large value of  $t_\perp^0$  deduced from band structure calculations, the fact that  $t_\perp(\mathbf{k})$  is minimum at the nodes may explain why the  $c$ -axis coherence appears only at very low temperature. Conversely, if one assumes that  $t_\perp^0$  is strongly renormalized (by electron-electron interaction for instance) in comparison to the band structure calculations value, the  $c$ -axis coherence is a consequence of electronic states at the anti-node. ARPES measurements in overdoped  $\text{Bi}_2\text{Sr}_2\text{CaCu}_2\text{O}_{8+\delta}$  [24] and in underdoped  $\text{YBa}_2\text{Cu}_3\text{O}_y$  [25, 26] have shown that  $t_\perp$  (connected with the bilayer effect) is strongly suppressed in comparison with the band structure calculations value. This argues for the second scenario, where those states at  $(\pi, 0)$  are in fact the small closed pocket responsible for the oscillations.

In this scenario, the presence of electronic states at the anti-node is difficult to reconcile with the observation of Fermi arcs in ARPES measurements above  $T_c$  in underdoped cuprates [27]. However, the observation of quantum oscillations has revealed that the FS of underdoped  $\text{YBa}_2\text{Cu}_3\text{O}_y$  undergoes a profound transformation at low temperature. This interpretation has been recently strengthened by nuclear magnetic resonance (NMR) measurements [18] showing that the translational

symmetry of the  $\text{CuO}_2$  planes in  $\text{YBa}_2\text{Cu}_3\text{O}_y$  is broken by the emergence of a unidirectional modulation of the charge density at a temperature  $T_{\text{charge}} = 50 \pm 10$  K for  $p=0.108$  and above a threshold field  $B \approx 20$  T.  $T_{\text{charge}}$  deduced from NMR measurement coincides roughly with the temperature  $T_0$ , the temperature at which  $R_H(T)$  changes sign. Combined with the evidence that this pocket is electron-like [9, 10, 16, 17], its location at  $(\pi, 0)$ , where most density-wave scenarios predict the emergence of such a pocket (see for example refs 28–30), greatly strengthens the case for FS reconstruction in  $\text{YBa}_2\text{Cu}_3\text{O}_y$ .

Although recent specific heat [31] and Seebeck coefficient [17] measured at high fields point to a Fermi surface made of only one pocket [32], the emergence of a strong MR at low temperature is naturally explained by the FS reconstruction into electron and hole sheets, due to the ambipolar character of the Fermi surface. In Fig. 3 we compare the slope of the magnetoresistance  $\rho_c(B)$  and the in-plane Hall coefficient  $R_H$  as a function of temperature measured at the same hole doping. The onset of the MR in  $\rho_c$  coincides with the FS reconstruction thus revealing the two roles played by the electron pocket: it enhances the orbital MR due to in-plane motion of carriers and it allows that the MR to be reflected in inter-plane transport.

It now becomes necessary to deduce the MR-free temperature dependence of  $\rho_c(T)$  by extrapolating the in-field resistivity  $\rho_c(B)$  to  $B = 0$ , defined as  $\rho_c(0)$ . Since a strong MR develops at low temperature, any smooth extrapolation to  $B = 0$  will give the same trend for the temperature dependence of  $\rho_c(0)$ , namely an initial rise with decreasing temperature turning into a drop at low temperature. To illustrate this, we extrapolate the in-field resistivity  $\rho_c(B)$  to  $B = 0$  using the same two-band model (electron and hole carriers) that self-consistently accounted for the temperature and field dependence of the longitudinal and transverse (Hall) resistivities of  $\text{YBa}_2\text{Cu}_4\text{O}_8$  [33]. Fitting every isotherm down to 10 K in Fig. 1 (dashed lines) yields the extrapolated zero-field resistivity  $\rho_c(0)$  shown in green open squares in Fig. 2. The initial rise in  $\rho_c(0)$  with decreasing temperature turns into a drop at low temperature, passing through a maximum at  $T_{\text{coh}} = 27 \pm 3$  K. This is in reasonable agreement with the energy scale  $t_\perp \approx 15$  K obtained from the splitting of frequencies in quantum oscillations for  $\text{YBa}_2\text{Cu}_3\text{O}_y$  at  $p = 0.10 - 0.11$  [12, 14]. The same analysis for the two other compositions are shown in the supplementary material [20] and yields  $T_{\text{coh}} = 20 \pm 5$  K for  $p = 0.097$  and  $T_{\text{coh}} = 35 \pm 5$  K for  $p = 0.12$ .

Several models based on incoherent tunneling between layers, assisted by interplanar disorder, have been invoked to explain the anomalous  $c$ -axis transport in cuprates (see ref 7 and ref. therein). However, several experimental facts demonstrate that the coherent  $c$ -axis transport at low temperature is a direct consequence of

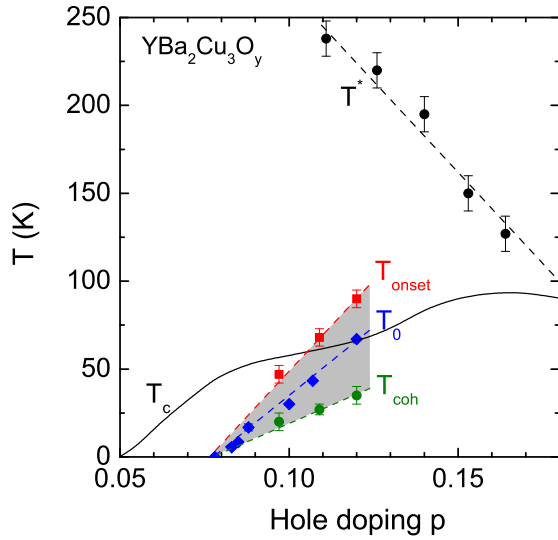


FIG. 4: (color on line) Temperature-doping phase diagram of  $\text{YBa}_2\text{Cu}_3\text{O}_y$ , with the superconducting phase in zero magnetic field delineated by the transition temperature  $T_c$ . Black circles mark the temperature  $T^*$  below which the in-plane resistivity deviates from its linear temperature dependence at high temperature (from data in ref. 37), a standard definition for the onset of the pseudogap phase. The onset of coherence in the  $c$ -axis resistivity at  $T_{\text{onset}}$  (red squares) is plotted along  $T_{\text{coh}}$  (green circles), the temperature where  $\rho_c(T)$  peaks (see Fig. 2 and ref. 20). The coherence crossover splits the phase diagram into two regions: an incoherent 2D regime above and a coherent 3D regime below.  $T_0$  is the temperature at which the normal-state in-plane Hall coefficient  $R_H(T)$  of  $\text{YBa}_2\text{Cu}_3\text{O}_y$  changes sign from positive at high temperature to negative at low temperature (blue diamonds; from ref. 16)

the Fermi surface reconstruction occurring at a temperature scale  $T_{\text{charge}} \approx T_0$ . From  $c$ -axis transport measurements, we define  $T_{\text{onset}}$  as the temperature below which  $\rho_c$  starts deviating from its  $1/T$  dependence at high temperature and  $T_{\text{coh}}$  as the characteristic temperature for the crossover to the coherent regime at which  $\rho_c(0)$  peaks (see Fig. 2). In Fig. 4, we compare these temperatures as a function of doping on the phase diagram of  $\text{YBa}_2\text{Cu}_3\text{O}_y$ . Not only do the two phenomena start at the same temperature for a given doping, they also trend similarly as a function of doping, both decreasing to lower  $T$  with decreasing  $p$ . In addition, these characteristic temperatures extrapolate to zero at lower doping  $p \approx 0.08$ , where  $R_H(T)$  no longer shows any downturn (see data for sample with  $T_c = 44.5$  K in ref. 16). This qualitative change has been attributed to the disappearance of the electron pocket, either caused by a Lifshitz transition [16] or by a phase transition [34]. Earlier measurements of  $c$ -axis transport on a sample with  $T_c = 49$  K [21] are consistent with such a transition: the MR in  $\rho_c(T)$  is entirely gone and  $\rho_c$  is now incoherent, increasing down to the lowest temperatures.

A natural explanation of our results is to invoke an

electron pocket at the anti-nodal position when the Fermi surface reconstruction occurs. Between the pseudogap temperature  $T^*$  and the temperature characteristic of the FS reconstruction  $T_0$ , the lack of well-defined quasiparticle peak seen by ARPES in the anti-nodal regions leads to a semiconducting-like behavior in  $\rho_c$ . The emergence of a unidirectional modulation of the charge density seen by high-field NMR in YBCO [18] and the similarity in the thermoelectric transport properties of  $\text{YBa}_2\text{Cu}_3\text{O}_y$  and  $\text{La}_{1.8-x}\text{Eu}_{0.2}\text{Sr}_x\text{CuO}_4$  [17] - a cuprate where stripe order is well-established from X-ray diffraction [35] - argue for a charge-stripe order causing the reconstruction of the FS at low temperature for  $p > 0.08$ . The resulting FS contains at least a high-mobility electron pocket, which produces a metallic-like transport in the plane and along the  $c$ -axis at low temperature. The electron pocket disappears below  $p \approx 0.08$ , probably because of a transition from a charge-stripe order ( $p > 0.08$ ) to a phase with spin order ( $p < 0.08$ ) [36]. In the absence of this electron pocket, both in-plane and out-of-plane transport properties are incoherent at low temperature.

We thank A. Carrington, S. Chakravarty, A. Chubukov, M. H. Julien, S. Kivelson, A. Millis, M. Norman, R. Ramazashvili, T. Senthil, G. Rikken and M. Vojta for useful discussions. Research support was provided by the French ANR DELICE, Euromagnet II, the Canadian Institute for Advanced Research and the Natural Science and Engineering Research Council.

\* Electronic address: cyril.proust@lncmi.cnrs.fr

- [1] S. L. Cooper and K. E. Gray, *Physical properties of high temperature superconductors IV* (World Scientific, Singapore, vol IV, 1994).
- [2] D. G. Clarke and S. P. Strong, *Adv. Phys.* **46**, 545 (1997).
- [3] N. E. Hussey, *Handbook of high-temperature superconductivity* (Springer 2007).
- [4] D. N. Basov and T. Timusk, *Rev. Mod. Phys.* **77**, 721 (2005).
- [5] T. Timusk and B. Statt, *Rep. Prog. Phys.* **62**, 61 (1999).
- [6] P.W. Anderson, *Science* **256**, 1526 (1992).
- [7] D. B. Gutman and D. L. Maslov, *Phys. Rev. Lett.* **100**, 047004 (2008).
- [8] N. Doiron-Leyraud *et al.*, *Nature* **447**, 565 (2007).
- [9] D. LeBoeuf *et al.*, *Nature* **450**, 533 (2007).
- [10] J. Chang *et al.*, *Phys. Rev. Lett.* **104**, 057005 (2010).
- [11] B. Vignolle *et al.*, *Nature* **455**, 952 (2008).
- [12] A. Audouard *et al.*, *Phys. Rev. Lett.* **103**, 157003 (2009).
- [13] S. E. Sebastian *et al.*, *Phys. Rev. B* **81**, 214524 (2010).
- [14] B. J. Ramshaw *et al.*, *Nature Physics* **7**, 234 (2011).
- [15] O. K. Andersen *et al.*, *J. Phys. Chem. Solids* **56**, 1573 (1995).
- [16] D. LeBoeuf *et al.*, *Phys. Rev. B* **83**, 054506 (2011).
- [17] F. Laliberté *et al.*, *Nature Comm.* (in press), arXiv: 1102.0984 (2011).
- [18] T. Wu *et al.*, preprint (2011).
- [19] L. B. Ioffe and A. J. Millis, *Phys. Rev. B* **58**, 11631

- (1998).
- [20] See supplementary material.
  - [21] F. F. Balakirev *et al.*, Physica C **341-348**, 1877 (2000).
  - [22] N. E. Hussey *et al.*, Nature **425**, 814 (2003).
  - [23] S. Chakravarty *et al.*, Science **261**, 337 (1993).
  - [24] D. L. Feng *et al.*, Phys. Rev. Lett. **86**, 5550 (2001).
  - [25] D. Fournier *et al.*, Nature Physics **6**, 905 (2010).
  - [26] Y. Sassa *et al.*, Phys. Rev. B **83**, 140511(R) (2011).
  - [27] M.R. Norman *et al.*, Nature **392**, 157 (1998).
  - [28] A.J. Millis and M. Norman, Phys. Rev. B **76**, 220503(R) (2007).
  - [29] S. Chakravarty and H.-Y. Kee, PNAS **105**, 8835 (2008).
  - [30] H. Yao *et al.*, arXiv: 1103.2115 (2011).
  - [31] S. C. Riggs *et al.*, Nature Physics **7**, 332 (2011).
  - [32] N. Harrison and S. E. Sebastian, Phys. Rev. Lett. **106**, 226402 (2011).
  - [33] P. M. C. Rourke *et al.*, Phys. Rev. B **82**, 020514(R) (2010).
  - [34] S. E. Sebastian *et al.*, Proc. Natl Acad. Sci. USA **107**, 6175 (2010).
  - [35] J. Fink *et al.*, Phys. Rev. B **83**, 092503 (2011).
  - [36] D. Haug *et al.*, New J. of Phys. **12**, 105006 (2010).
  - [37] Y. Ando *et al.*, Phys. Rev. Lett. **93**, 267001 (2004).
  - [38] To compare  $\Delta F$  in ref. [12] and ref. [14], one should multiply the latter by a factor 2 because of the different notation.

# Supplementary material for "Coherent $c$ -axis transport in the underdoped cuprate superconductor $\text{YBa}_2\text{Cu}_3\text{O}_y$ "

## SAMPLE PREPARATION AND EXPERIMENTAL SETUP

The samples studied were single crystals of  $\text{YBa}_2\text{Cu}_3\text{O}_y$ , grown in non-reactive  $\text{BaZrO}_3$  crucibles from high-purity starting materials and subsequently detwinned. The doping  $p$  of each crystal was inferred from its superconducting transition temperature  $T_c$  [1]. Electrical contacts to the sample were made by evaporating gold, with large current pads and small voltage pads mounted across the top and bottom so as to short out any in-plane current (Corbino geometry). Several samples of different thicknesses were measured, each giving similar values of the absolute  $c$ -axis resistivity. The resistivity was measured at the LNCMI in Toulouse, in pulsed magnetic fields up to 60 T. A current excitation of 5 mA at  $\approx 60$  kHz was used. The voltage (and a reference signal) was digitized using a high-speed digitizer and post-analysed to perform the phase comparison.

## C-AXIS MAGNETORESISTANCE AT DIFFERENT DOPING LEVEL

Fig. 1a and Fig. 1b present the longitudinal  $c$ -axis resistivity up to 60 T for two other underdoped samples of  $\text{YBa}_2\text{Cu}_3\text{O}_y$  at a hole doping  $p=0.097$  ( $T_c=57.0$  K) and  $p=0.120$  ( $T_c=66.4$  K), respectively. Similarly to the  $p=0.109$  sample, a strong positive magnetoresistance grows with decreasing temperature below 60 K and the in-field  $c$ -axis resistivity increases down to about 4 K, followed by a saturation at lower temperature.

## FLUX FLOW CONTRIBUTION TO THE RESISTIVITY

Upon cooling, the resistivity drops because of superconductivity. This drop starts at lower temperature for higher fields. We define the threshold field beyond which the normal state is reached as the field for which  $\rho_c(T)$  shows no drop. To confirm that this saturation of  $\rho_c(T)$  at low temperature is not due to some compensation between superconducting drop and insulating-like normal-state resistivity, we show that the saturation persists at fields above the threshold field (see Fig. 2). In all three samples, 50 T is above the threshold field down to the lowest temperatures. Therefore the magnetoresistance

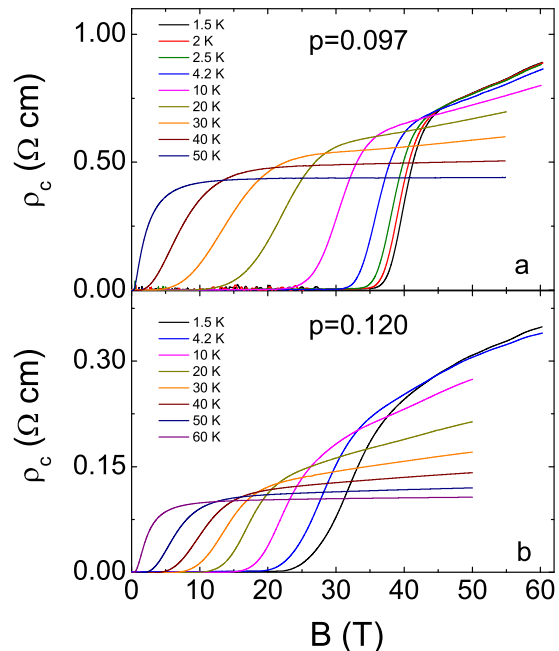


FIG. 1: Electrical resistivity  $\rho_c$  of  $\text{YBa}_2\text{Cu}_3\text{O}_y$ : (a)  $p=0.097$  and (b)  $p=0.120$  for a current  $I$  and a magnetic field  $B$  along the  $c$  axis ( $I \parallel B \parallel c$ ) at different temperatures below  $T_c$ .

measured at 50 T is purely a normal-state property, at all three dopings.

The Nernst effect is a sensitive probe of flux flow, because moving vortices make a large positive contribution to the Nernst coefficient. In Fig. 3, we compare the field dependence of the in-plane Hall coefficient [2] and  $c$ -axis resistivity with that of the Nernst coefficient measured in  $\text{YBa}_2\text{Cu}_3\text{O}_y$  at  $p = 0.12$  and  $T = 10$  K [3]. The Nernst coefficient develops a strong positive peak above the melting line due to vortex motion in the vortex liquid phase and is followed by a gradual descent to negative values (the quasiparticle contribution) until it becomes almost flat as the field approaches 30 T. This saturation is best captured by the field derivative of the Nernst coefficient shown by a red line in Fig. 3a. Above the threshold field of about 30 T, the Hall coefficient becomes flat (as indicated by the blue dashed line in Fig. 3b) and the two-band model used to fit the normal state  $c$ -axis resistivity merges with the data (see Fig. 3c). This comparison confirms that flux-flow contribution to the normal-state transport is negligible for fields greater than 30 T at this doping level (and temperature). Therefore, the magnetoresistance above 30 T is entirely due to quasiparticles,



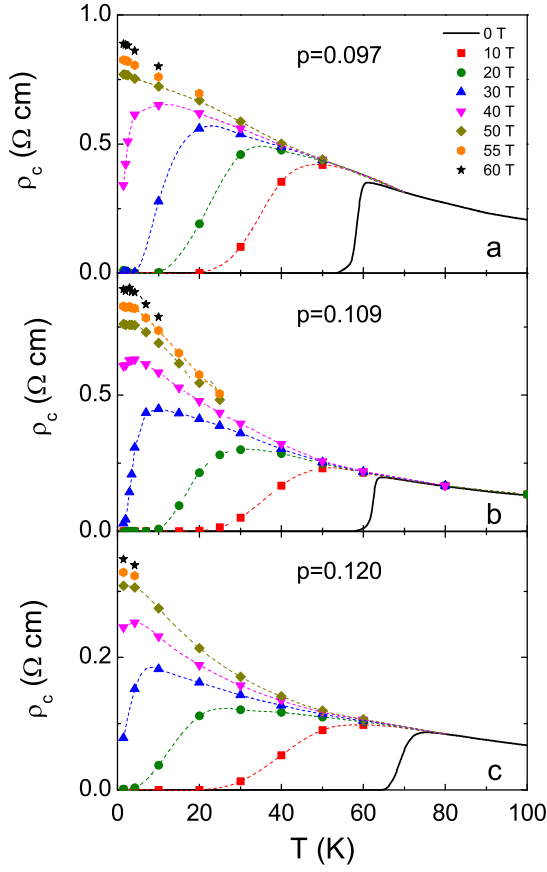


FIG. 2: Electrical resistivity  $\rho_c$  of  $\text{YBa}_2\text{Cu}_3\text{O}_y$ : (a)  $p = 0.097$ , (b)  $p = 0.109$  and (c)  $p = 0.120$  plotted as a function of temperature for different values of the magnetic field. Dashed lines are a guide to the eye. The increase of the in-field c-axis resistivity down to about 4 K is in part due to the strong magnetoresistance which develops at temperature below 60 K.

demonstrating that the  $\rho_c(0)$  values deduced from the fits are a property of the normal state.

In the supplementary information of ref. 2, the field scale above which the effects of vortex motion and superconducting fluctuations have become negligible in  $R_{xx}$  and  $R_{xy}$ , have been determined such that these transport coefficients reflect predominantly the properties of the normal state.  $T_0(B)$  is the temperature at which  $R_H(T)$  changes sign. The key observation is that  $T_0$  is independent of field at the highest fields (up to 60 T) in three materials ( $p=0.10-0.14$ ). This shows that the temperature-induced sign change in  $R_H$  at high fields is not caused by flux flow and is thus clearly a property of the normal state. The case is particularly clear in the  $p = 0.120$  sample, where the sign change occurs above  $T_c(0)$  and is totally independent of field over the entire field range from 0 to 45 T. In addition flux flow yields a contribution to the Hall resistance which is strongly non-linear in  $B$ , so that the Hall coefficient should depend strongly on magnetic field. This is not the case for the three samples

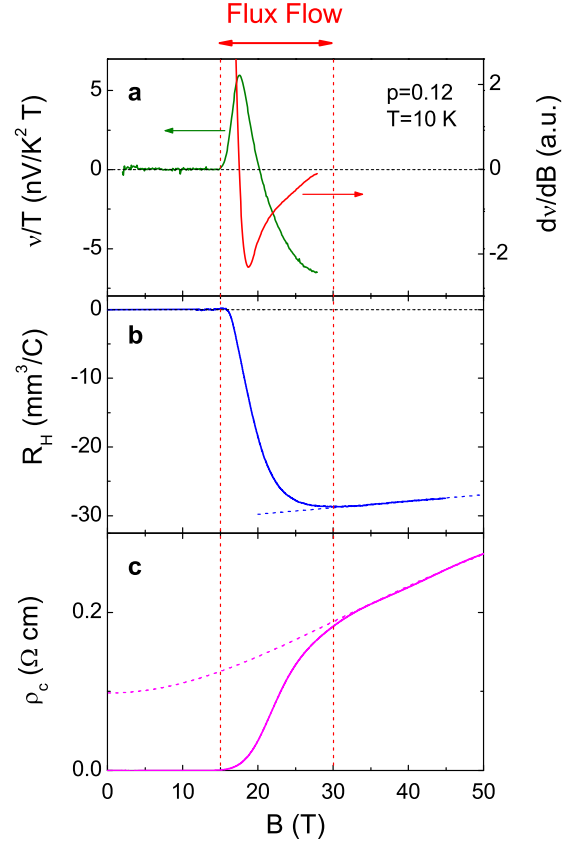


FIG. 3: Field dependence of (a) the Nernst coefficient [3], (b) the Hall coefficient [2] and (c) the c-axis resistivity (Fig. 1c) of YBCO at  $p = 0.12$  and  $T = 10$  K. Above a threshold field of about 30 T (indicated by the right vertical dashed red line), the Nernst coefficient  $\nu$  (panel a; green curve) saturates to its negative quasiparticle value, as demonstrated by its derivative (panel a; red curve) which goes to zero as  $B \approx 30$  T. This saturation shows that the positive contribution to the Nernst coefficient from superconducting fluctuations has become negligible above 30 T. Above this field, the Hall coefficient is almost flat (dashed blue line in panel b) and the two-band model fit to the c-axis resistivity (dashed magenta line in panel c) merges with the data. We conclude that at 10 K and above 30 T the flux-flow contribution to the transport properties is negligible, and the large magnetoresistance at high field is purely a property of the normal state.

at the highest fields, where  $R_H$  is flat. This is further evidence that we are probing the normal state properties of these compounds in the field/temperature range. Earlier high-field measurements of  $\rho_c$  in  $\text{YBa}_2\text{Cu}_3\text{O}_y$  [4] show a striking difference between the large magnetoresistance observed in samples with  $T_c = 60$  K and the absence of the magnetoresistance in sample with  $T_c = 49$  K. This can only be due to normal state transport properties and can be explained by the vanishing of the very mobile electron pocket for the low doping sample [5]. There is no alternative explanation in term of flux flow.

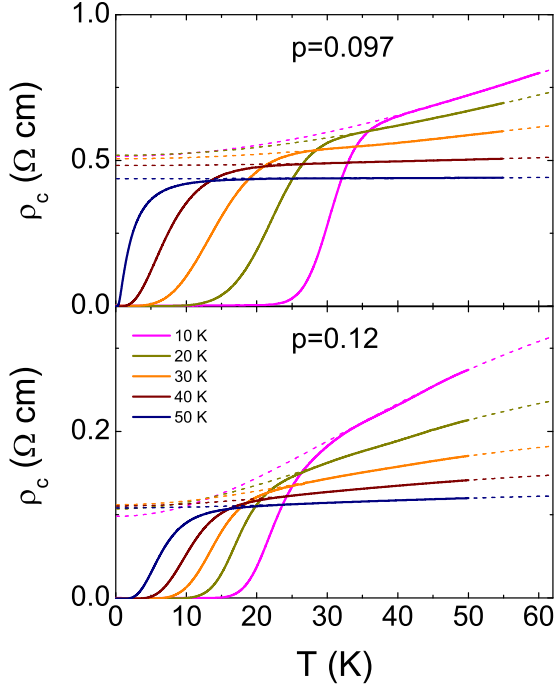


FIG. 4: The raw resistivity curves of Fig. 1 are fitted using the two-band model (see text). The dashed lines are a fit of each isotherm to Eq. 1 above the superconducting transition for (a)  $p = 0.097$ , (b)  $p = 0.120$ . The parameter  $\rho_0$  gives the zero-field extrapolation  $\rho_c(0)$ , plotted in Fig. 5.

### TWO-BAND MODEL

Assuming that the Fermi surface of underdoped  $\text{YBa}_2\text{Cu}_3\text{O}_y$  contains both electrons and holes, the transverse magnetoresistance can be fitted with a two-band model:

$$\rho(B) = \frac{(\sigma_h + \sigma_e) + \sigma_h \sigma_e (\sigma_h R_h^2 + \sigma_e R_e^2) B^2}{(\sigma_h + \sigma_e)^2 + \sigma_h^2 \sigma_e^2 (R_h + R_e)^2 B^2} = \rho_0 + \frac{\alpha B^2}{1 + \beta B^2} \quad (1)$$

$\sigma_h$  ( $\sigma_e$ ) is the conductivity of holes (electrons) and  $R_h$  ( $R_e$ ) is the Hall coefficient for hole (electron) carriers. Using the three free parameters  $\rho_0$ ,  $\alpha$  and  $\beta$ , we were able to subtract the orbital magnetoresistance from the field sweeps and get the temperature dependence of the zero-field resistivity  $\rho_c(0) = \rho_0(T)$ . In order to estimate error bars, we fitted each field sweep data set to eq. 1 between a lower bound  $B_{\text{cut-off}}$  and the maximum field strength and monitored the value of  $\rho_c(0)$  as a function of  $B_{\text{cut-off}}$ . The resulting fits to  $\rho_c(B)$  at different temperatures for the samples  $p = 0.097$  and  $p = 0.120$  are shown in Fig. 4.

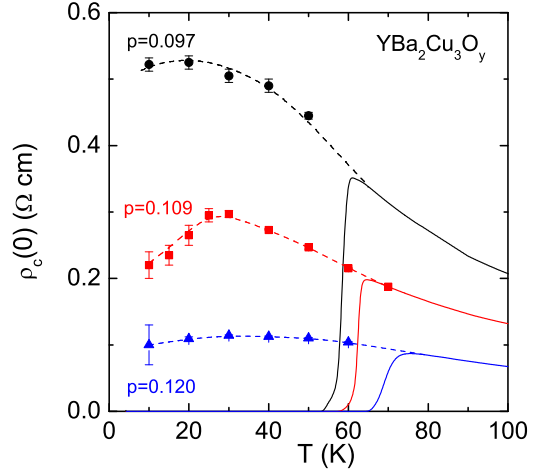


FIG. 5: Temperature dependence of the  $c$ -axis resistivity of  $\text{YBa}_2\text{Cu}_3\text{O}_y$  from which the magnetoresistance has been subtracted using a two-band model (see text).

### TEMPERATURE DEPENDENCE OF THE ZERO-FIELD EXTRAPOLATED RESISTIVITY

Fig. 5 shows the temperature dependence of the  $c$ -axis resistivity of  $\text{YBa}_2\text{Cu}_3\text{O}_y$  from which the magnetoresistance has been subtracted using a two-band model (Eq. 1) to extrapolate the normal-state data to  $B = 0$ , for the three samples, as labelled. Solid lines show the resistivity measured in zero magnetic field. Dashed lines are a guide to the eye. The onset of this crossover occurs at a temperature  $T_{\text{onset}}$ , below which the zero-field  $c$ -axis resistivity  $\rho_c(0)$  deviates downward from its  $1/T$  dependence at high temperature. A characteristic temperature for the crossover between incoherent  $c$ -axis transport at high temperature and coherent transport at low temperature is the temperature at which  $\rho_c(0)$  peaks, with values  $T_{\text{coh}} = 20, 27$  and  $35$  K for  $p = 0.097, 0.109$  and  $0.120$  respectively. This is in reasonable agreement with the energy scale  $t_{\perp} \approx 15$  K obtained from the splitting of frequencies in quantum oscillations for  $\text{YBa}_2\text{Cu}_3\text{O}_y$  at  $p = 0.10 - 0.11$  [6].

\* Electronic address: cyril.proust@lncmi.cnrs.fr

- [1] R. Liang *et al.*, Phys. Rev. B **73**, 180505(R) (2006).
- [2] D. LeBoeuf *et al.*, Nature **450**, 533 (2007).
- [3] J. Chang *et al.*, Phys. Rev. Lett. **104**, 057005 (2010).
- [4] F. F. Balakirev *et al.*, Physica C **341-348**, 1877 (2000).
- [5] D. LeBoeuf *et al.*, Phys. Rev. B **83**, 054506 (2011).
- [6] A. Audouard *et al.*, Phys. Rev. Lett. **103**, 157003 (2009).